International Journal of Thermophysics, Vol. 27, No. 3, May 2006 (© 2006)
DOI: 10.1007/s10765-006-0055-0

Measurement and Modeling of the Bidirectional Reflectance of SiO_2 Coated Si Surfaces

H. J. Lee[1] and Z. M. Zhang[1,2]

Received September 7, 2005

An understanding of the variation of directional radiative properties of rough surfaces with dielectric coatings is important for temperature measurements and heat transfer analysis in many industrial processes. An experimental study has been conducted to investigate the effect of coating thickness on the bidirectional reflectance distribution function (BRDF) of rough silicon surfaces. Silicon dioxide films with thicknesses of 107.2, 216.5, and 324.6 nm were deposited using plasma-enhanced chemical vapor deposition onto the rough side of two Si wafers. The wafer surfaces exhibit distinct anisotropic characteristics as a result of chemical etching during the manufacturing process. A laser scatterometer measures the BRDF at a wavelength of 635 nm, after improvement of the signal-to-noise ratio. The slope distribution function obtained from the measured BRDF of uncoated Si surfaces was used in an analytical model based on geometric optics for rough surface scattering and thin-film optics for microfacet reflectance. The predicted BRDFs are in reasonable agreement with experimental results for a large range of coating thicknesses. The limitations of the geometric optics for modeling the BRDF of coated anisotropic rough surfaces in the specular direction are demonstrated. The results may benefit future radiative transfer analysis involving complicated surface microstructures with thin-film coatings.

KEY WORDS: bidirectional reflectance distribution function (BRDF); radiative properties; rough surfaces; thin films.

1. INTRODUCTION

The bidirectional reflectance, formally known as the bidirectional reflectance distribution function (BRDF), is a fundamental radiative property, which describes the redistribution of energy reflected from a rough

[1] The George W. Woodruff School of Mechanical Engineering, Georgia Institute of Technology, Atlanta, Georgia 30332, U.S.A.
[2] To whom correspondence should be addressed. E-mail: zhuomin.zhang@me.gatech.edu.

0195-928X/06/0500-0820/0 © 2006 Springer Science+Business Media, Inc.

surface [1]. Knowledge of BRDFs is essential for radiative heat transfer analysis between rough surfaces. For example, radiation thermometers are commonly used in rapid thermal processing to monitor the wafer temperature by measuring the spectral radiance from the back side of the wafer [2]. It is crucial to determine the effective emissivity and the BRDF of microrough Si surfaces, which are often coated with thin oxides. Because thin films on a surface can change the directional and spectral reflectance considerably [1–3], a number of studies have been devoted to the study of BRDFs of rough surfaces with thin-film coatings [4–11]. Lu et al. [4] numerically solved the electromagnetic wave equations to obtain the scattered fields from one-dimensional and perfectly conducting rough surfaces with a dielectric film. Gu et al. [5] compared numerical solutions with experimental measurements for scattering from dielectric substrates with a dielectric film. Because the computation for rigorous solutions is too long and/or too expensive for practical applications, various approximate methods have also been developed to model the BRDF of coated rough surfaces, such as the perturbation theory [6], Kirchhoff's approximation [7], and the geometric optics approximation (GOA) [8–10].

Despite the strong dependence of the reflectance on film thickness, very few studies have paid attention to the change of BRDF with film thickness. Tang et al. [8] extended the GOA by incorporating thin-film optics to account for the reflectance change due to the coating. Zhu et al. [9] compared this hybrid modeling with rigorous solutions to investigate its validity numerically. In these studies, the rough surface statistics were assumed to be Gaussian and isotropic. Strong anisotropy in the roughness statistics were observed in some silicon wafers after chemical etching [11,12]. The present study focuses on systematic investigations of the effect of the film thickness on the BRDF of anisotropic rough surfaces with thin-film coatings. A laser scatterometer was used to measure the BRDF of anisotropic microrough Si surfaces with SiO_2 coatings. An effort was made to develop a simple model that can capture the scattering behavior of anisotropic surfaces with coatings. The slope distribution function (SDF) obtained from the measured BRDF of uncoated surfaces was imported to model the BRDF of coated surfaces. Experimental and predicted results are compared to quantitatively examine the variation of BRDF with coating thickness.

2. EXPERIMENTS

The substrates used in the present study are two Si wafers (Si-1 and Si-2) with different surface roughness characteristics, as reported in previous studies [11,12]. Both wafers are single-side polished, lightly doped

⟨100⟩ single-crystal silicon. The surface topography of the rough side of the wafers was characterized with an atomic force microscope (AFM). The height distribution functions of Si-1 and Si-2 are non-Gaussian with small negative skewness. The rms roughness (σ) of Si-1 is $0.51 \pm 0.03\,\mu$m, and that of Si-2 is $0.63 \pm 0.04\,\mu$m. The height distribution functions of the two samples resemble each other and deviate slightly from a Gaussian function. However, SDFs of Si-1 and Si-2 are anisotropic and exhibit a four-fold symmetry. While the SDF of Si-1 has a single dominant peak and is slightly anisotropic, the SDF of Si-2 exhibits strong anisotropy as evidenced by the large and small side peaks in addition to a dominant peak at the center. Detailed descriptions and important characteristic roughness parameters of the two surfaces can be found in Ref. 11 and will not be repeated here.

The 100-mm diameter Si wafers, Si-1 and Si-2, were cut into 25 mm × 25 mm square specimens. The rough side of the specimens was coated with a SiO_2 film by a plasma-enhanced chemical vapor depositor (PEC-VD). The rough surfaces were placed into the deposition chamber together with several small pieces of smooth Si surfaces. This way, the same coating thickness was applied to different specimens. The same procedure was repeated with different deposition time to obtain three different coating thicknesses.

A schematic of the coated rough surface and the coordinates for the BRDF are shown in Fig. 1. The (average) coating thickness h is assumed to be the same as the film thickness on the smooth reference samples. Coating thicknesses were measured at 20 different points on the reference samples with a Nanospec 3000 optical profilometer made by Nanometrics Inc. This optical profilometer measures the reflectance in a wavelength range from 400 to 800 nm, and the measured reflectance is fitted with an analytical formula by adjusting the phase shift between the two return beams: one from the film-substrate interface and the other from the air-film interface. The coating thickness can be determined using the measured phase shift of the reflected light in combination with the known refractive index of the film. The measured SiO_2 coating thicknesses are 107.2 ± 0.3 nm, 216.5 ± 0.5 nm, and 324.6 ± 2.1 nm, with a reproducibility of 0.2 nm.

A laser scatterometer, specifically the three-axis automated scatterometer (TAAS) [13], was used to measure the BRDF of the samples. Figure 2 shows a schematic of the optical setup of the TAAS. The sample is vertically mounted. Three rotary stages, automatically controlled by a computer, are used to change incidence and reflection directions. One rotates the sample around the y axis to change the incidence angle θ_i, another rotates detector A in the x–z (horizontal) plane to change the reflection

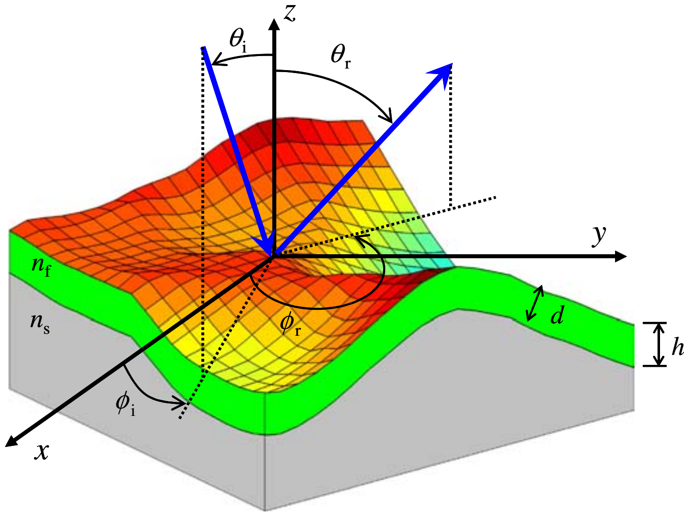

Fig. 1. Schematic of the BRDF of a thin-film coated rough surface. Here, x, y, and z are the global coordinates, where the x-y plane is the mean surface of the air-SiO_2 interface. θ_i and ϕ_i are the zenith and azimuthal angles of incidence, whereas θ_r and ϕ_r are the zenith and azimuthal angles of reflection, respectively. The refractive index of the coating is n_f and that of the substrate is n_s. The substrate is thick enough to be treated as semi-infinite. The average thickness of the coating is h, and $d = h \cos \alpha$ is the local film thickness. It is assumed that h is uniform, and thus the profile for the air-SiO_2 interface is identical to that of the SiO_2-Si interface.

angle θ_r, and the third rotates the arm of detector A out of the x–z plane to change the azimuthal angle ϕ_r. Manual rotation of the sample on a sample holder around the z axis adjusts the azimuthal angle ϕ_i. The incident laser beam is parallel to the optical table (x-z plane). A diode laser system serves as an optical source, and a lock-in amplifier connected with a diode laser controller modulates the output optical power at 400 Hz. In the present study, a diode laser at 635 nm wavelength was used. The diode laser is mounted on a thermoelectrically controlled stage to provide power stability within a standard deviation of 0.2%. An optical fiber is used to provide flexibility for optical access and alignment. The light from the output end of the fiber is in the horizontal plane. As shown in Fig. 2, the beam first passes through a collimator consisting of a lens and a small aperture. A linear polarizer mounted on a dial allows the selection of polarization for light incident on the sample. The beamsplitter then divides the laser beam into two passes: one goes to the sample and the

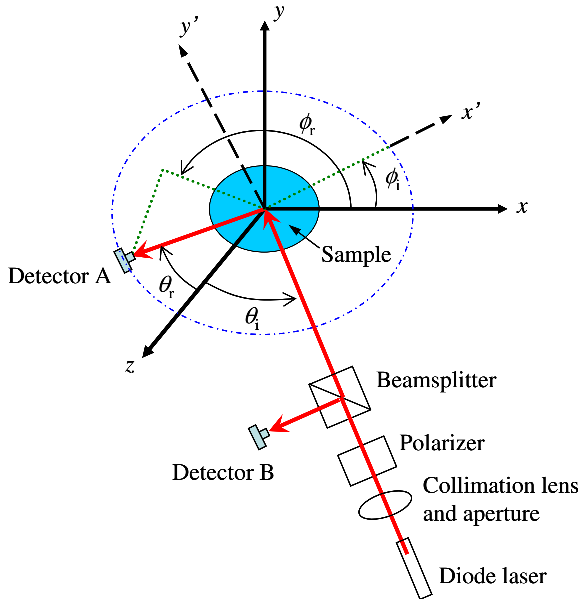

Fig. 2. Schematic of TAAS for BRDF measurements. Here, a sample is vertically mounted, and the laser beam is parallel to the optical table, which is in the x–z plane. Rotating the sample around the y axis changes θ_i, and rotating detector A in the x–z plane changes θ_r. ϕ_i can be changed by rotating the sample around the z axis. To measure the in-plane BRDF, the detector is kept within the horizontal plane.

other to a stationary reference detector B. The light scattered by the sample is measured by detector A. The power collected at each detector is sent to two trans-impedance pre-amplifiers with nine decades of amplification range. The pre-amplifier has a linear frequency response from DC up to a certaint maximum frequency that is much greater than 400 Hz. The lock-in amplifier only picks up the phase-locked signals at 400 Hz, thereby eliminating the effect of background radiation or stray light without using a chopper. The measurement equation for the BRDF is given by

$$f_r(\theta_i, \phi_i, \theta_r, \phi_r) = C_I \frac{V_A}{V_B \cos\theta_r \Delta\omega_r} \tag{1}$$

where V_A and V_B are outputs of detectors A and B, respectively, and $\Delta\omega_r$ is the reflection solid angle, which is 1.84×10^{-4} sr as determined by the area of a precision-machined aperture in front of the detector and

the distance between this aperture and the beam spot on the sample. An instrument constant C_I compensates the beamsplitter ratio and the difference in the responsivities of the two detectors. The BRDF within $\pm 2.5°$ of the retroreflection direction ($\theta_r = \theta_i$ and $\phi_r = \phi_i$) cannot be measured since the movable detector blocks the incident beam. In all BRDF measurements, V_A and V_B are averaged over ten measurements at a given position to reduce the random error. The relative uncertainty of TAAS is estimated to be 5% for the BRDF greater than 0.1 by intercomparison with a reference standard instrument [13].

The output power from the diode laser after the optical fiber is usually less than 2 mW. The collimation lens and aperture reduce the optical power by approximately 50%. The beamsplitter has a transmittance of near 50%. The polarizer has a transmittance of 20% for incidence that is randomly polarized or linearly polarized at 45° with respect to the selected polarization (0° and 90° for *s* and *p* polarization, respectively). In previous measurements, the power reaching the sample could be as low as 0.05 mW for certain polarization. Because the coated surfaces have a much smaller reflectance than the uncoated Si surfaces due to the reduction of reflectance by the low refractive index film, similarly to the antireflection effect [14], the reflected power reaching detector A can be very low. If the signal is too weak compared to the noise level, the measurement standard deviation can be very large, resulting in random fluctuations in the BRDF values. As an example, Fig. 3 shows the measured BRDF of Si-1 coated with a SiO_2 film of $h = 107.2$ nm at normal incidence for *s* polarization. In the earlier measurement, the measured BRDF value fluctuated when $f_r \cos\theta_r$ was less than 0.04 due to the large standard deviation. In the present study, the reported BRDF results are always given as $f_r \cos\theta_r$, and are based on the average of ten consecutive measurements. A procedure was developed to enhance the signal level in the measurements of small BRDFs as explained below.

In earlier measurements, the gain was set to be the same for all θ_r values. In order to take full advantage of the dynamic range of pre-amplifiers, manual adjustment is necessary for large θ_r when the reflected power is small. The gain ratio has been carefully calibrated and shown to be linear. The use of a large gain can provide sufficient signal to the lock-in amplifier, which will filter out the noise from the phase-locked signal. Notice that the output of the diode laser is linearly polarized, but the orientation of polarization at the output end of the optical fiber depends on how the fiber is positioned. Therefore, the linear polarizer is essential to provide either *s*- or *p*-polarized light to the sample. When the polarization of the diode laser is parallel to that of the polarizer, the output power is maximized for a given polarization but minimized for the other.

In previous measurements, an effort was made to position the fiber such that the power reaching the sample would be approximately equal when the linear polarizer is rotated between 0° and 90° to switch the polarization state. In the present study, however, the laser power is maximized for individual polarization by repositioning the optical fiber each time when the polarizer is rotated. It should be emphasized that the polarization state of the laser coming out from the fiber affects the signal-to-noise ratio but does not affect the actual polarization of the light reaching the sample. Once the fiber position is fixed, the laser output is very stable in terms of both the power and polarization. Furthermore, the original beamsplitter with a transmittance of about 50% was replaced with one that has a transmittance greater than 90%. The improvement of the signal-to-noise ratio, by properly selecting the pre-amplifier gain and optimizing the optical efficiency of the laser power to the sample, has resulted in a much lower standard deviation, which is approximately 10% when $f_r \cos\theta_r = 0.001$, as can be seen from Fig. 3. Further investigation confirmed that the relative standard deviation is less than 1% when $f_r \cos\theta_r > 0.01$ and less than 10% when $f_r \cos\theta_r > 0.001$.

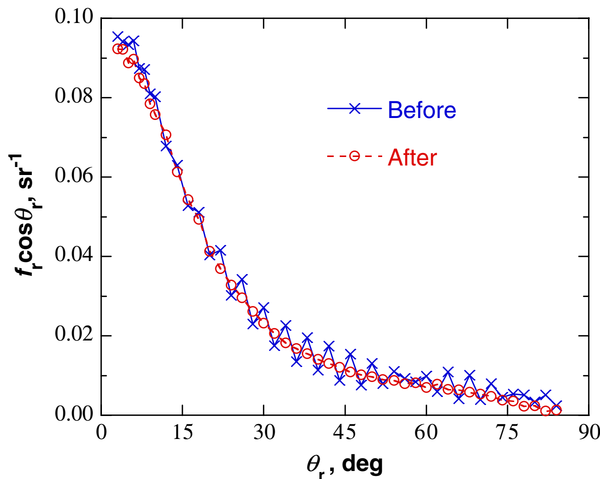

Fig. 3. Illustration of the effectiveness of the procedure used to improve the signal-to-noise ratio for the BRDF measurement of a coated Si-1 sample with a 107.2 nm SiO_2 film. Before: measurements taken earlier without applying the procedure; after: results after reduction of the standard deviation.

3. ANALYTICAL MODELING

Based on GOA, the BRDF can be calculated with analytical models or Monte Carlo ray-tracing methods. Analytical models allow one to conveniently calculate the BRDF [15–19]. Most analytical models account for only first-order scattering whereas a few consider multiple scattering, which is significant at large angles of incidence or reflection. Because multiple scattering involves shadowing and re-striking (masking), additional assumptions must be made in order to obtain analytical expressions. For two-dimensional (2-D) surfaces, multiple scattering is accompanied by the change of the polarization state upon reflection. Very few analytical models simultaneously consider multiple scattering and the change of the polarization state. On the other hand, the Monte Carlo methods [8–11,20] can be used to model multiple scattering and account for the change in the polarization state, but require much more computation time and resources [11]. Lee et al. [11] showed that multiple scattering is negligible for Si-1 and Si-2 at incidence angles up to 45°. Thus, the present study will simply adopt an analytical model to study the BRDF of coated surfaces without considering multiple scattering.

For the in-plane BRDF ($\phi_r = \phi_i$ or $\phi_r = \phi_i + 180°$), Zhu and Zhang [21] unified several analytical models considering first-order scattering only. Their expression is given as follows:

$$f_r(\theta_i, \phi_i, \theta_r, \phi_r) = \frac{p(\zeta_x, \zeta_y) S(\theta_i, \sigma/\tau) S(\theta_r, \sigma/\tau)}{4\cos\theta_i \cos\theta_r \cos^4\alpha} \rho(n, \psi) \tag{2}$$

Here, ζ_x and ζ_y in the SDF $p(\zeta_x, \zeta_y)$ are the slopes in the x and y directions, given by

$$\zeta_x = \frac{\partial \zeta}{\partial x} = -\frac{\sin\theta_i \cos\phi_i + \sin\theta_r \cos\phi_r}{\cos\theta_i + \cos\theta_r} \tag{3a}$$

and

$$\zeta_y = \frac{\partial \zeta}{\partial y} = -\frac{\sin\theta_i \sin\phi_i + \sin\theta_r \sin\phi_r}{\cos\theta_i + \cos\theta_r}, \tag{3b}$$

respectively. To account for shadowing and re-striking, the Smith shadowing function S is used, which is a function of the incidence or reflection zenith angle and the ratio of the rms roughness to the autocorrelation length (σ/τ) [22]. The microfacet reflectance $\rho(n, \psi)$, where n is a complex refractive index and ψ is the local incidence angle, is calculated from Fresnel's reflection coefficients by averaging over the two polarizations. In the denominator of Eq. (2), α is the inclination angle of the microfacet.

While $\alpha = (\theta_i + \theta_r)/2$ and $\psi = |\theta_i - \theta_r|/2$ for $\phi_r = \phi_i$, $\alpha = |\theta_i - \theta_r|/2$ and $\psi = (\theta_i + \theta_r)/2$ for $\phi_r = \phi_i + 180°$.

If the coating is sufficiently thin and of uniform thickness, the microfacet reflectance ρ can be calculated from Airy's formula considering multiple reflections and interferences inside the film as [1]

$$\rho(n_f, n_s, \beta) = \left| \frac{r_{0f} + r_{fs} e^{-i2\beta}}{1 + r_{0f} r_{fs} e^{-i2\beta}} \right|^2 \quad (4)$$

In the above expression, r_{0f} and r_{fs} are Fresnel's reflection coefficients at the air-film and film-substrate interfaces, respectively. The phase shift for a wave traveling through the film is

$$\beta = \frac{2\pi n_f d \cos\theta_f}{\lambda} \quad (5)$$

where θ_f is the refraction angle in the film, defined in the local coordinates of a microfacet, and λ is the wavelength in vacuum. Since the microfacet is tilted by an inclination angle α, the local film thickness d is the projection of h to the microfacet normal, hence, $d = h\cos\alpha$. In addition to the assumption of uniform film thickness on each microfacet, the application of Eq. (4) also implies that the microfacet is sufficiently large compared with film thickness and the autocorrelation length is much larger than the rms roughness. Otherwise, the reflected waves by different microfacets may interfere with each other. Zhu et al. [9] regarded this phenomenon as the corner effect, which will be significant for the very precipitous surface, relatively thick coatings, or at large incidence/reflection angles.

For a Gaussian surface, only the rms slope (w) is needed to determine $p(\zeta_x, \zeta_y)$. Because Si-1 and Si-2 cannot be modeled as Gaussian surfaces and Si-2 is strongly anisotropic, their SDFs cannot be expressed with simple functions. Accordingly, a large number of surface topographic measurements are required for obtaining a reliable SDF. Previous comparisons for Si-1 and Si-2 based on surface topographic measurements showed that the artifacts of AFM measurements could cause discrepancies between the predicted and measured BRDFs [11,12]. It is difficult, however, to distinguish whether the modeling error comes from the SDF based on the topographic measurements or from the failure of GOA. If the same approach based on the measured surface topography were applied to model the BRDF of coated surfaces in the present study, the modeled BRDFs would be subjected to three potential errors: imperfect surface characterization, the inherent limitation of GOA for rough surfaces without coating, and the additional limitation of GOA due to coating. A new modeling approach, which uses the SDF extracted from the BRDF of bare Si surfaces with an inverse method

rather than that obtained from the measured surface topography, is proposed. This approach is free from the error of surface characterization and less time-consuming.

The inverse method calculates the cross section of the 2-D SDF from a known in-plane BRDF [12]. Since Si-1 and Si-2 have anisotropic SDFs, the in-plane BRDF depends on the variation of ϕ_i, which can be treated by rotating the SDF. The rotational transform of coordinates ζ_x and ζ_y by ϕ_i can be performed using the following expressions:

$$\zeta_{x'} = \zeta_x \cos\phi_i + \zeta_y \sin\phi_i \quad (6a)$$

$$\zeta_{y'} = \zeta_y \cos\phi_i - \zeta_x \sin\phi_i \quad (6b)$$

After the SDF is transformed to the new coordinates, $\zeta_{x'}$ and $\zeta_{y'}$, one can set $\zeta_{y'} = 0$ to obtain the cross section corresponding to the in-plane BRDF at ϕ_i as follows.

$$p(\zeta_{x'}, \zeta_{y'} = 0) = \frac{4 f_r(\theta_i, \phi_i, \theta_r; \phi_r) \cos\theta_i \cos\theta_r \cos^4\alpha}{S(\theta_i, \sigma/\tau)\, S(\theta_r, \sigma/\tau)\, \rho(n_s, \psi)} \quad (7)$$

Since the ratio σ/τ should be known prior to determining $S(\theta_i, \sigma/\tau)$ and $S(\theta_r, \sigma/\tau)$, iteration is required for evaluating Eq. (7). When the BRDF measured at normal incidence is used, the effect of the shadowing function can be minimized. For isotropic surfaces, the cross section of SDF, $p(\zeta_{x'}, \zeta_{y'} = 0)$, from the measured in-plane BRDF for any azimuthal angle suffices to determine σ/τ. However, for anisotropic surfaces, the 2-D SDF should be obtained from the BRDF measured over the hemisphere. The out-of-plane measurement over the entire hemisphere is extremely time-consuming and not very practical. An alternative method to determine σ/τ is to regard it as a fitting parameter. After obtaining the cross section of SDF from the in-plane BRDF at normal incidence with Eq. (7), the in-plane BRDF at oblique incidence calculated with Eq. (2) can be fit to measurements by changing the parameter σ/τ. However, the ratios σ/τ obtained from the AFM measurement [11] ($\sigma/\tau = 0.51/4.34 = 0.12$ for Si-1 and $\sigma/\tau = 0.63/3.05 = 0.21$ for Si-2) were imported in the present study after assuming that the difference in σ/τ between measured and iteratively calculated values is negligible. Because the BRDF around the retroreflection direction cannot be measured with TAAS, the SDF from the BRDF measured at $\theta_i = 3°$ is used to patch the SDF within $0° \leqslant \theta_r \leqslant 2°$.

For comparison purposes, the cross sections of the SDF obtained from both AFM and BRDF measurements are shown in Fig. 4. The AFM results for $\zeta_x = 0$ correspond to the BRDF results for $\phi_i = 0°$, and the AFM results for $\zeta_x = \zeta_y$ correspond to the BRDF results for $\phi_i = 45°$.

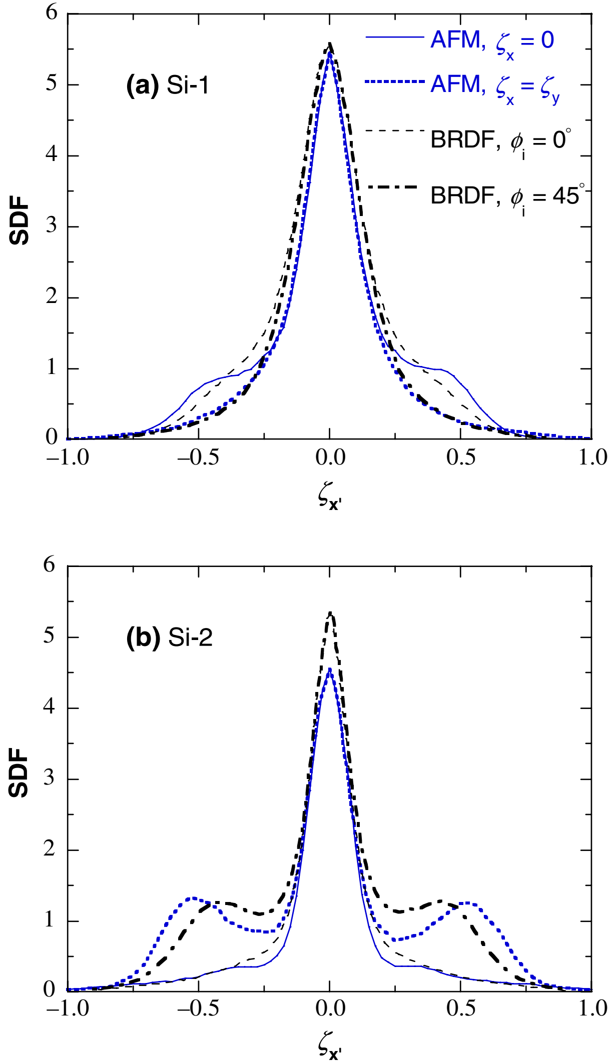

Fig. 4. Cross sections of the SDF obtained from AFM and BRDF measurements for bare silicon samples (a) Si-1 and (b) Si-2 at two different azimuthal angles.

The cross sections obtained from the two methods have the same trend. The difference is large for Si-2 around the specular peak ($\theta_r = \theta_i$ and $\phi_r = \phi_i$) and side peaks. By using the cross sections of the SDF obtained

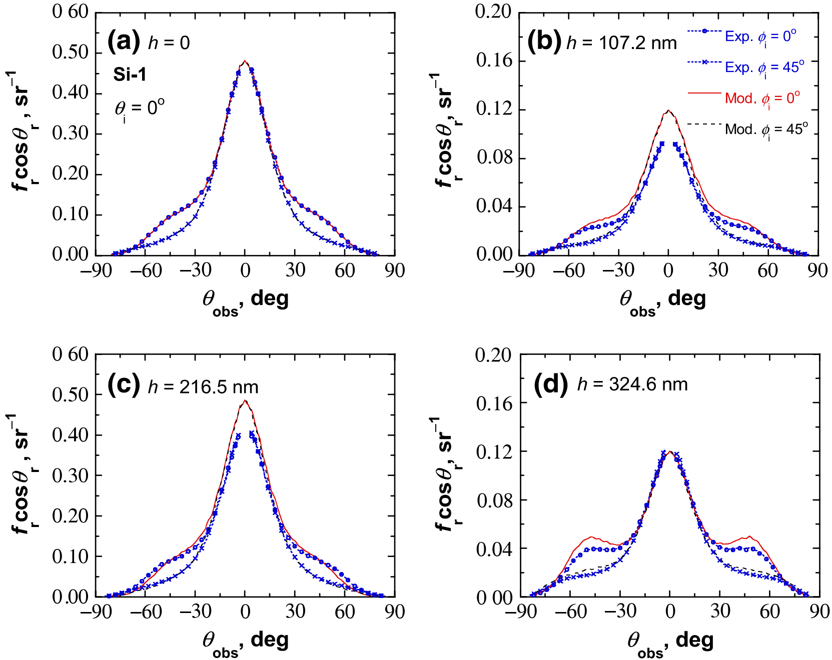

Fig. 5. Comparison of the measured and predicted BRDFs for Si-1 for random polarization at $\theta_i = 0°$ with different coating thicknesses: (a) $h = 0$; (b) $h = 107.2$ nm; (c) $h = 216.5$ nm; (d) $h = 324.6$ nm.

inversely from BRDF measurements, the effect of AFM artifacts is eliminated in the present study.

4. RESULTS

The BRDF of Si-1 at normal incidence is shown in Fig. 5 for different coating thicknesses, where the results are averaged over s and p polarizations. The complex refractive indices of Si and SiO_2 are (3.882, 0.019) and (1.457, 0), respectively, at the laser wavelength $\lambda = 635$ nm [23]. Because of beam blocking, no data are available within $\pm 2.5°$ of the retroreflection direction ($\theta_{obs} = -\theta_i$). The observation angle θ_{obs} is defined as θ_r when $\phi_r = \phi_i + 180°$ and $-\theta_r$ when $\phi_r = \phi_i$. In the legend, abbreviations of "Exp" and "Mod" stand for experimental and modeling results, respectively. When the measurements were repeated for the same sample after remounting, the standard deviation is within 5% for $f_r \cos\theta_r > 0.01$. This is consistent with an earlier estimate of the uncertainty of

the instrument based on comparisons with a standard instrument at the National Institute of Standards and Technology (NIST). Note that experimental and modeling results are exactly the same when $h = 0$ because the cross sections of the SDF are obtained from the BRDF of the bare Si surface. The predicted results agree well with measurements for all thicknesses. The BRDFs of coated surfaces reveal similar anisotropic features to those observed without coating while the predicted BRDF in Fig. 5d shows a much more distinct shoulder. The BRDFs around the specular direction ($\theta_{obs} = \theta_i$) depend little on ϕ_i, and the disagreement between measurement and prediction is large at $h = 107.2$ nm and $h = 216.5$ nm.

Figure 5 shows that the magnitude of the BRDF changes significantly with film thickness. The measured BRDF values around the specular direction in Fig. 5b,d are reduced by approximately four times, compared to those in Fig. 5a, whereas the reduction in Fig. 5c is insignificant. The change of the BRDF can be explained by the variation of the phase shift β with film thickness. If a surface is smooth, the phase shifts β at normal incidence are 88.5°, 178.8°, and 268.1° for film thicknesses of 107.2, 216.5, and 324.6 nm, respectively. While the local refraction angle is generally nonzero for a rough surface, the normal vector of microfacets is only slightly perturbed from that of a mean plane due to the small rms slope of Si-1. When β is close to 90° ($h = 107.2$ nm) and 270° ($h = 324.6$ nm), destructive interferences within the coating result in a reduction of the microfacet reflectance and BRDF. On the contrary, when β is close to 180° ($h = 216.5$ nm), constructive interferences prevail and the BRDF values in Fig. 5c are comparable to that of the bare Si surface. The GOA modeling is expected to be invalid as h becomes very large, due to the corner effect. However, the agreement at $h = 324.6$ nm is not the worst. This counter-intuitive result may be related to the interference between scattered waves, which may be dependent on film thickness.

Figure 6 shows a similar comparison made with Si-2, whose SDF is strongly anisotropic and exhibits two side peaks along the diagonal directions in the SDF as can be seen from Fig. 4. The side peaks in the slope distribution bring about counterparts in the BRDF at approximately $\theta_r = 50°$. While the central peak is much larger in the left panels, the side peaks are more prominent in the right panels. Figure 6b,c shows that the GOA model agrees with the experiment at large reflection angles but significantly overpredicts BRDFs when $\theta_r \leqslant 15°$. The agreement is the worst for $h = 324.6$ nm, and the prediction is significantly lower than the measurement for $\theta_r \leqslant 45°$. Because the microfacets of Si-2 are more precipitous than those of Si-1, the corner effect for such a coating thickness may be significant and responsible for the large disagreement seen in Fig. 6d. In addition to the corner effect, the profile of the air-film interface may differ

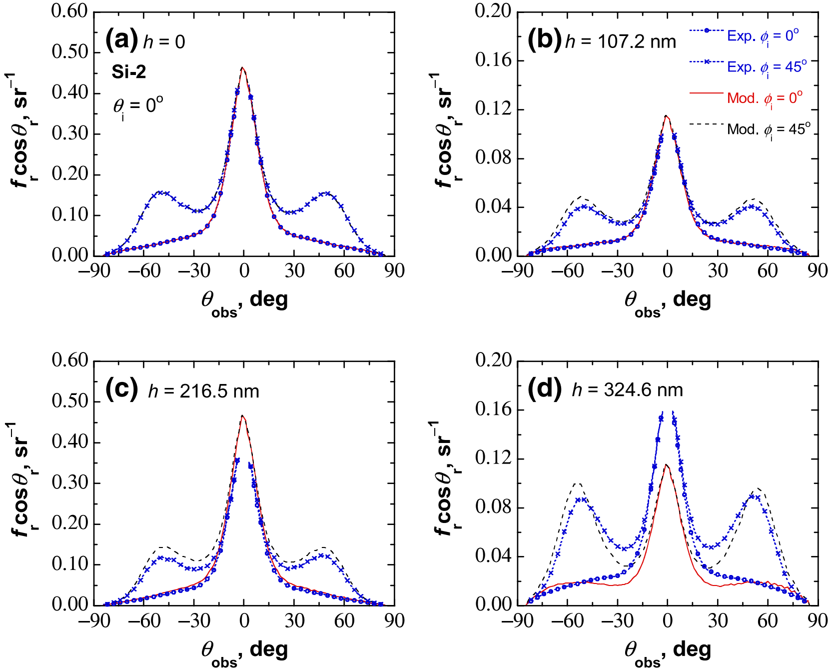

Fig. 6. Comparison of the measured and predicted BRDFs for Si-2 for random polarization at $\theta_i = 0°$ with different coating thicknesses: (a) $h = 0$; (b) $h = 107.2$ nm; (c) $h = 216.5$ nm; (d) $h = 324.6$ nm.

from that of the film-substrate interface. The interface variation is more likely to take place at a rougher surface and with a larger coating thickness. Since it was demonstrated that the roughness statistics of approximately 100 nm thick gold coatings are essentially the same as those of bare substrates, only the topography of Si surfaces with 216.5 and 324.6 nm thick SiO_2 coatings was measured three times each with the previously used AFM [11]. The averaged rms roughness σ and rms slope w of Si-1 are 0.51 and 0.29 when $h = 216.5$ nm while $\sigma = 0.52$ and $w = 0.28$ when $h = 324.6$ nm. Since $\sigma = 0.51 \pm 0.03$ and $w = 0.28 \pm 0.01$ for bare Si-1, a uniform coating thickness is a good assumption for Si-1. However, the averaged σ and w of Si-2 seem to increase gradually with h. When $h = 216.5$ nm, $\sigma = 0.65$ and $w = 0.50$. When $h = 324.6$ nm, $\sigma = 0.69$ and $w = 0.52$, which is slightly beyond their ranges for bare Si-2 ($\sigma = 0.63 \pm 0.04$ and $w = 0.47 \pm 0.04$). Consequently, the large disparity observed in Fig. 6d may be attributed to the corner effect and non-uniform coating thickness.

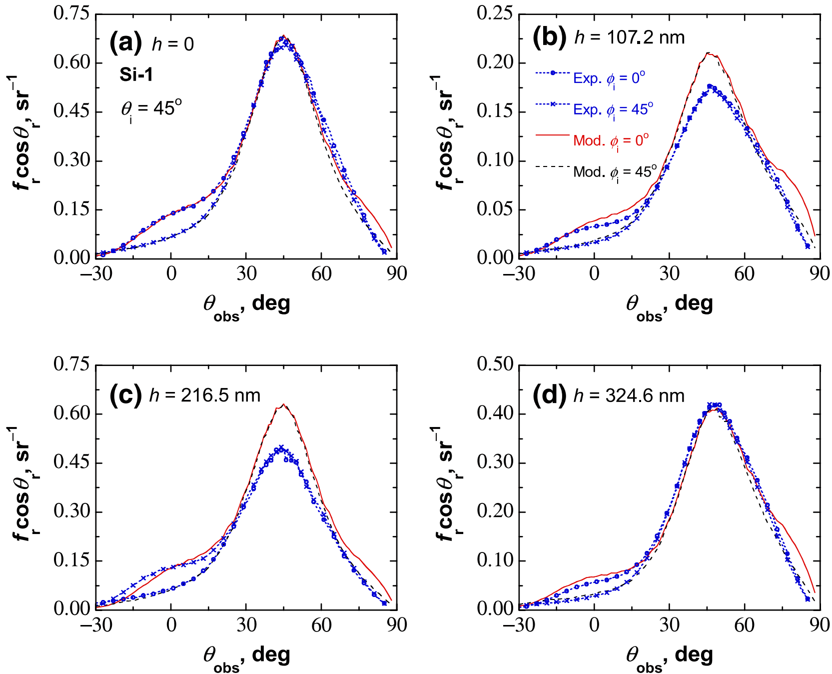

Fig. 7. Comparison of the measured and predicted BRDFs for Si-2 for random polarization at $\theta_i = 45°$ with different coating thicknesses: (a) $h = 0$; (b) $h = 107.2\,\text{nm}$; (c) $h = 216.5\,\text{nm}$; (d) $h = 324.6\,\text{nm}$.

The BRDF of Si-1 at $\theta_i = 45°$ is shown in Fig. 7 to investigate the BRDF at oblique incidence. The predicted BRDFs at $\theta_{obs} > 50°$ in Fig. 7a exhibit deviations from the measured values. The GOA modeling is often inaccurate at large reflection angles due to multiple scattering and interference between scattered waves. Because the former is negligible, the latter is likely to be responsible for the deviations. When the coating exists, the deviation along $\phi_i = 0°$ is more distinct. Note that for Si-1 without coatings, the predicted BRDF using the SDF obtained from AFM measurements showed similar deviations at large reflection angles, especially for *s* polarization [11,12]. Similarly to the results shown in Fig. 5, the BRDFs in the left panels are larger than those in the right panels. The reduction of the BRDF in Fig. 7d is not as significant as that in Fig. 5d. Because of the $\cos\theta_f$ term in Eq. (5), the phase shift β at $\theta_i = 45°$ is 234.4°, which deviates from 270°. The disagreement around the specular direction is also obvious when $h = 107.2\,\text{nm}$ and $h = 216.5\,\text{nm}$. Again, a larger film thickness does not always result in a larger disagreement.

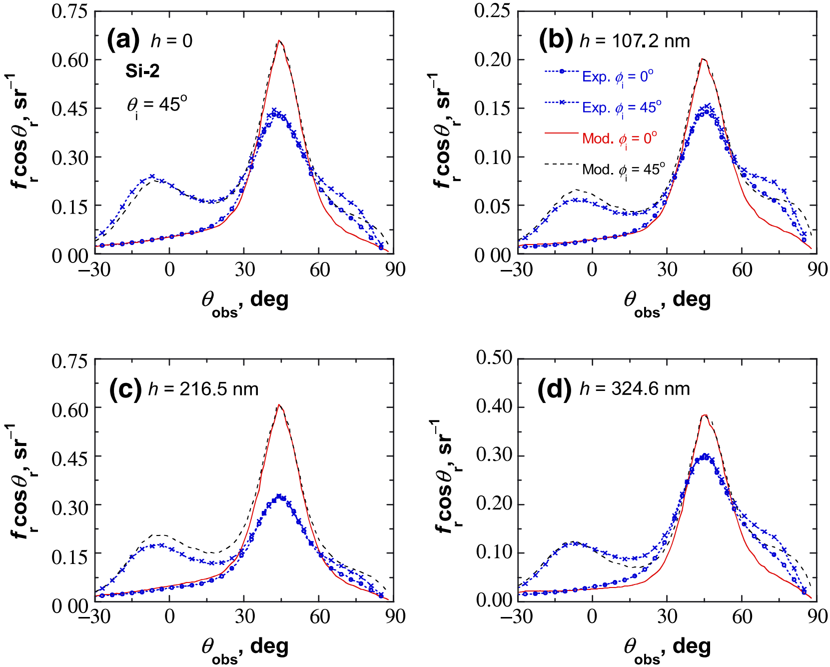

Fig. 8. Comparison of the measured and predicted BRDFs for Si-1 for random polarization at $\theta_i = 45°$ with different coating thicknesses: (a) $h = 0$; (b) $h = 107.2$ nm; (c) $h = 216.5$ nm; (d) $h = 324.6$ nm.

Figure 8 shows the BRDF of Si-2 at $\theta_i = 45°$. There exists a large disagreement around the specular direction and at large reflection angles even without coating as can be seen from Fig. 8a. GOA becomes invalid as the optical roughness, defined as $\sigma \cos\theta_i/\lambda$, decreases [20]. Thus, because the optical roughness at $\theta_i = 45°$ is smaller than that at $\theta_i = 0°$, the large disagreement occurs. Nevertheless, the prediction at $\theta_i = 45°$ for Si-2 is worse than that for Si-1, especially around the specular direction, because the ratio σ/τ of Si-2 is larger ($\sigma/\tau = 0.12$ for Si-1 and $\sigma/\tau = 0.21$ for Si-2). Tang et al. [20] suggested the validity regime of GOA as $\sigma \cos\theta_i/\lambda > 0.2$ at $\sigma/\tau = 0.21$ for a 1-D perfectly conducting surface. Although Si-2 is within the validity regime of GOA ($\sigma \cos\theta_i/\lambda = 0.7$), it does not ensure good agreement since this regime may not be applicable for a dielectric surface with strong anisotropy such as Si-2. Considering the large disagreement for Si-2 without coating, the additional disagreement caused by coating does not seem as significant. Rather, the predicted and measured BRDFs in Fig. 8b,c,d agree better than those in Fig. 8a in some

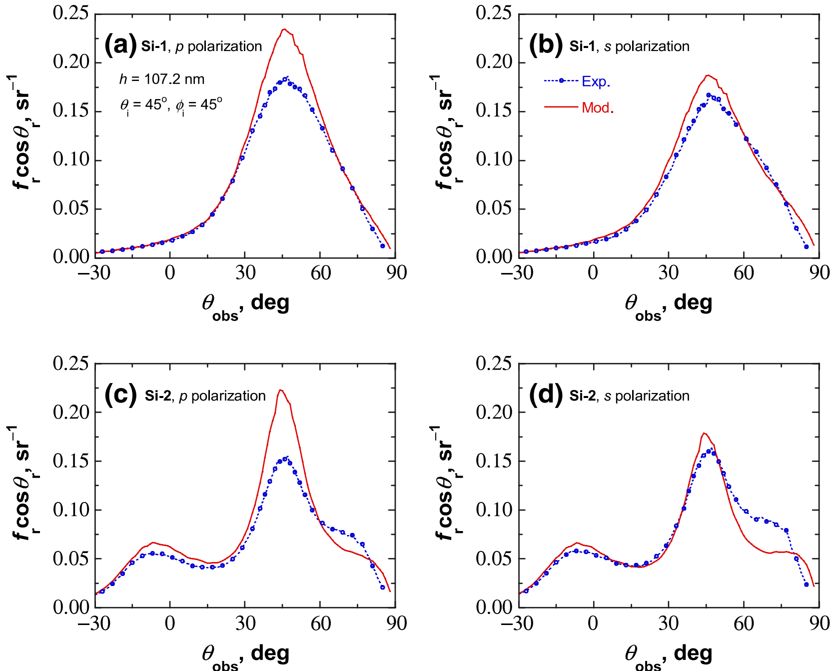

Fig. 9. Comparison of the measured and predicted BRDFs with a coating thickness $h = 107.2\,\text{nm}$ at $\theta_i = 45^\circ$ and $\phi_i = 45^\circ$: (a) Si-1 and p polarization; (b) Si-1 and s polarization; (c) Si-2 and p polarization; (d) Si-2 and s polarization.

regions. For example, the modeled BRDF in Fig. 8c agrees better with experiment at $\theta_{obs} \leqslant -10^\circ$ and large θ_{obs}. The relative error at the specular peak is reduced from 53% at $h = 0$ to 35% at $h = 107.2\,\text{nm}$ or to 24% at $h = 324.6\,\text{nm}$. The modeling results for $h = 324.6\,\text{nm}$ have already a large disagreement at $\theta_i = 0^\circ$ as shown in Fig. 6d. The disagreement at $\theta_i = 45^\circ$ does not increase much, as can be seen from Fig. 8d, although the corner effect is expected to be more significant at oblique incidence [9]. Better agreement for coated surfaces at $\theta_i = 45^\circ$ may be attributed to complicated counteraction among the inherent limitation of GOA, the corner effect, and non-uniform coating thickness.

Because the BRDF depends on the incidence polarization, results are presented for each polarization in Fig. 9 obtained at $\theta_i = 45^\circ$ and $\phi_i = 45^\circ$ when $h = 107.2\,\text{nm}$. If Si-1 and Si-2 without coating are studied for the same incidence angle, the BRDF for s polarization is much greater than that for p polarization because of the greater microfacet reflectance ρ. However, the measured BRDFs for two polarizations are comparable

to each other with the presence of coating. Measurement shows that the BRDF of Si-1 around the specular peak for p polarization is slightly larger than that for s polarization. However, the comparison between two polarizations for Si-2 shows the opposite. Within the GOA domain, the BRDF is proportional to the microfacet reflectance ρ according to Eq. (2). For a microfacet that is parallel to the mean plane (zero slope), ρ for p or s polarization is 0.119 or 0.095, respectively, with $\theta_i = 45°$. Therefore, the predicted BRDF around the specular peak for p polarization is greater for both Si-1 and Si-2. The comparison in Fig. 9 demonstrates that there is a case where the BRDF of coated surfaces cannot be explained with GOA, even in a qualitative manner, when the BRDF for each polarization is compared.

5. CONCLUSION

The effect of film thickness on the BRDF of two anisotropic Si surfaces with SiO_2 films is investigated at three different thicknesses (107.2, 216.5, and 324.6 nm). Although the Si surfaces are coated with SiO_2, the underlying anisotropic features of Si substrates affect BRDF for all the studied thickness. Depending on film thickness, the SiO_2 coating can significantly reduce the BRDF. In the presence of a coating, the difference in the BRDF between p and s polarization decreases at oblique incidence. The modeling results are in reasonably good agreement with the measurements, also indicating the change of anisotropic BRDFs. This study suggests that GOA should be applicable for a large range of coating thickness: up to $h/\lambda \approx 0.5$ for Si-1 ($\sigma/\tau \approx 0.1$) and up to $h/\lambda \approx 0.3$ for Si-2 ($\sigma/\tau \approx 0.2$) at normal incidence. Additionally, a large coating thickness does not necessarily degrade modeling accuracy. Disagreement is more prominent around specular peaks and at large reflection angles, and it becomes larger for the sample with steep surface roughness (Si-2). This disagreement is presumably caused by the inherent limitation of GOA for rough surfaces without coating and the additional errors, which are made when the BRDF of the coated surfaces is modeled, such as the corner effect and non-uniform coating thickness. The present study on the effect of film thickness on the directional dependence of radiative properties of rough surfaces may benefit radiative heat transfer modeling for coated rough surfaces.

ACKNOWLEDGEMENTS

This work was supported by the National Science Foundation (CTS-0236831 and CTS-0500113). The authors thank Dr. Qunzhi Zhu and Mr. Yu-Bin Chen for helpful discussions.

NOMENCLATURE

d local film thickness
h (average) coating thickness
f_r bidirectional reflectance distribution function (BRDF)
n complex refractive index
p slope distribution function (SDF)
S Smith shadowing function
w root-mean-square slope

Greek symbols
α inclination angle
β phase shift
ζ microfacet slope
θ zenith angle
λ wavelength in vacuum
ρ microfacet reflectance
σ root-mean-square roughness
τ autocorrelation length
ϕ azimuthal angle
ψ local incidence angle
ω solid angle

Subscripts
0 air
f film
i incidence
obs observation
r reflection
s substrate

REFERENCES

1. M. F. Modest, *Radiative Heat Transfer* (McGraw-Hill, New York, 1993).
2. Z. M. Zhang, *Ann. Rev. Heat Transfer* **11**:351 (2000).
3. T. Makino, A. Nakamura, and H. Wakabayashi, *JSME Int. J. B* **42**:745 (1999).
4. J. Q. Lu, A. A. Maradudin, and T. Michel, *J. Opt. Soc. Am. B* **8**:311 (1991).
5. Z. H. Gu, J. Q. Lu, and A. A. Maradudin, *J. Opt. Soc. Am. A* **10**:1753 (1993).
6. J. M. Elson, *J. Opt. Soc. Am.* **67**:253 (1977).
7. T. R. Lettieri, E. Marx, J. F. Song, and T. V. Vorburger, *Appl. Opt.* **30**:4439 (1991).
8. K. Tang, P. A. Kawka, and R. O. Buckius, J. *Thermophys. Heat Transfer* **13**:169 (1999).
9. Q. Z. Zhu, H. J. Lee, and Z. M. Zhang, *J. Thermophys. Heat Transfer* **19**:548 (2005).
10. H. J. Lee, B. J. Lee, and Z. M. Zhang, *J. Quant. Spectrosc. Radiat. Transfer* **93**:185 (2005).
11. H. J. Lee, Y. B. Chen, and Z. M. Zhang, submitted to *Int. J. Heat Mass Transfer*.
12. Q. Z. Zhu and Z. M. Zhang, *Opt. Eng.* **44**:073601 (2005).

13. Y. J. Shen, Q. Z. Zhu, and Z. M. Zhang, *Rev. Sci. Instrum.* **74**:4885 (2003).
14. B. J. Lee, Z. M. Zhang, E. A. Early, D. P. DeWitt, and B. K. Tsai, *J. Thermophys. Heat Transfer* **19**:558 (2005).
15. K. E. Torrance and E. M. Sparrow, *J. Opt. Soc. Am.* **57**:1105 (1967).
16. L. Tsang and J. A. Kong, *J. Appl. Phys.* **51**:673 (1980).
17. J. J. Embrechts, *J. Sound Vib.* **229**:65 (2000).
18. K. Tang and R. O. Buckius, *Int. J. Heat Mass Transfer* **44**:4059 (2001).
19. J. Caron, J. Lafait, and C. Andraud, *Physica B* **325**:76 (2003).
20. K. Tang, R. A. Dimenna, and R. O. Buckius, *Int. J. Heat Mass Transfer* **40**:49 (1997).
21. Q. Z. Zhu and Z. M. Zhang, *J. Heat Transfer* **126**:985 (2004).
22. B. G. Smith, *IEEE Trans. Antennas Propag.* **15**:668 (1967).
23. E. D. Palik, *Handbook of Optical Constants of Solids* (Academic Press, Orlando, Florida, 1985).